ELSEVIER

Journal of Power Sources 106 (2002) 238–244

JOURNAL OF POWER SOURCES

www.elsevier.com/locate/jpowsour

Internal reforming of methane in solid oxide fuel cell systems

R. Peters*, R. Dahl, U. Klüttgen, C. Palm, D. Stolten

Institute for Materials and Processes in Energy Systems IWV 3, Energy Process Engineering, Forschungszentrum Jülich, D-52425 Jülich, Germany

Abstract

Internal reforming is an attractive option offering a significant cost reduction, higher efficiencies and faster load response of a solid oxide fuel cell (SOFC) power plant. However, complete internal reforming may lead to several problems which can be avoided with partial pre-reforming of natural gas. In order to achieve high total plant efficiency associated with low energy consumption and low investment costs, a process concept has been developed based on all the components of the SOFC system. In the case of anode gas recycling an internal steam circuit exists. This has the advantage that there is no need for an external steam generator and the steam concentration in the anode gas is reduced. However, anode gas recycling has to be proven by experiments in a pre-reformer and for internal reforming. The addition of carbon dioxide clearly shows a decrease in catalyst activity, while for temperatures higher than 1000 K hydrogen leads to an increase of the measured methane conversion rates.

Keywords: Steam reforming; Internal reforming; Solid oxide fuel cells; Natural gas; Anode gas recycling

1. Introduction

Fuel cells have the potential to become one of the most important energy conversion tools for the next century. Fuel cell technology shows advantages concerning fuel efficiency, emissions, maintenance and noise pollution. Fuel cell systems including peripherical components like fuel processors, heat exchangers and blowers, are under development for mobile, stationary and portable applications. For stationary applications, i.e. for power plants (300 MW_{el}) [1] or as combined heat and power generation [2] the solid oxide fuel cell (SOFC) is generally preferred. With respect to the production of heat and electricity in residential heating by fuel cell systems, more low-temperature (PEFC: polymer electrolyte fuel cell) than high-temperature fuel cells (SOFC, [3,4]) are under development. Also, it is being examined if the SOFC can be used in future as an auxiliary power unit (APU) in mobile applications [5] and for portable systems [6]. Some developers have recently announced preparations for pilot cell manufacturing [7,8]. SOFCs operate at temperatures between 973 and 1273 K using hydrogen-containing gas mixtures as the fuel, and oxygen in the air as the oxidant. At Forschungszentrum Jülich (FZJ) an anode-supported planar substrate concept has been developed [9] consisting of thin electrolyte films (10 μm) deposited on thick substrates (1.5–2 mm). The thin electrolyte allows operating temperatures between 973 and 1073 K and, thus the use of cheaper materials for the stack and the peripherical components compared to conventional systems with temperatures between 1223 and 1273 K. New developments in SOFC technology can be found in the literature [10–14].

The most interesting fuel for SOFC systems is natural gas consisting mainly of methane, i.e. 80–95% CH_4. The H_2/CO-rich gas used in the SOFC can be produced by heated steam reforming (HSR) [15–17] or by partial oxidation (POX) [18–20]. The POX process has advantages concerning start-up, load changes and the simpler set-up of the reformer. On the other hand, lower system efficiency and the low H_2 content in the reformat are drawbacks in comparison to steam reforming. Therefore, it is useful to apply the POX process in small systems like portables [6] and the steam reforming process in systems where high efficiencies are required.

The reforming process has to be adapted to the energy balance as part of the SOFC system. The FZJ concept is foreseen to perform the reforming process by two steps in different components, i.e. in a pre-reformer and within the anode chamber of the SOFC stack (internal reforming) [17]. The endothermic steam reforming of methane in the anode chamber is favourably applied to provide additional cooling of the cell and to reduce the expense of a pre-reformer. Because of higher hydrocarbons in natural gas, i.e. 5.5 (vol.%) C_2H_6, 1.3% C_3H_8, 0.5% C_4H_{10}, 0.1% C_5H_{12}, etc.

* Corresponding author. Tel.: +49-2461-61-4260; fax: +49-2461-61-8163.
E-mail address: ra.peters@fz-juelich.de (R. Peters).

0378-7753/02/$ – see front matter
PII: S0378-7753(01)01039-4

(rest: 88.3% methane, 3.0% nitrogen, 1.3% carbon dioxide), and several problems related to complete internal reforming a small pre-reformer for higher hydrocarbons has to be provided in future SOFC-plant concept development. More detailed information about the pre-reforming of natural gas is given by Peters et al. [21].

2. Internal steam reforming

Internal steam reforming has been discussed in the literature for providing additional cooling of the SOFC thereby reducing the amount of air passing to the cathode side of the fuel cell [16,17,22]. Generally, in a SOFC stack the temperature distribution resulting from the current density distribution, the gas flow distribution and the heat transfer has to be homogeneous both within the cell plane as well as perpendicular to the cell plane. Large temperature gradients in either direction can cause damage to one or more of the components or interfaces due to thermal stresses. The experiments on internal methane steam reforming have shown that the strong activity of the nickel anode results in a marked temperature reduction directly in the reaction zone. Since the associated temperature distribution cannot be tolerated in the SOFC stack, the reforming activity must be reduced by way of suitable measures. Several measures have been examined by experiments to optimise the catalyst activity and the flatness of the resulting temperature profile [23]. The SOFC-stack performance concerning temperatures, current densities, reaction zones and mechanical stresses on a local scale must be calculated by suitable models [24]. Kinetic models for the internal steam reforming of methane over nickel/zirconia were evaluated by different groups and can be found in the literature [25–28]. Several aspects of methane steam reforming over new materials like Ni on CGO were discussed in the literature [29–32].

In order to achieve a high total plant efficiency associated with low energy consumption and low investment costs, a process concept has been developed based on all the components of the SOFC system. One main target of further process development is to reduce the large amount of air supplied to the fuel cell stacks, which is necessary to remove the electrical waste heat. Plant optimisation requires a tool which takes the characteristic behaviour of the stack, its peripherical components and their interaction into account. The balance of plant calculations was performed by Riensche et al. [33,34] and Unverzagt [35] with a commercial flow sheet simulator (PRO/II, SimSci) for a decentralised natural-gas-fuelled SOFC power plant with 200 kW_{el} capacity. Starting from a basic plant concept with a simple flow sheet and a basic set of SOFC operation parameters, flow sheet and parameter variations were performed. One of the proposed flow sheets includes an anode gas recycling loop guiding part of the residual anode gas back in front of the pre-reformer. Besides some advantages concerning the recovering of waste heat and the operation parameters of the fuel cell, no external steam need to be produced. The amount of recycled anode gas is balanced in such a manner that steam for steam reforming is totally recovered from the SOFC. The flow sheet with anode gas recycling is discussed in more detail in [21]. Typically, the pre-reformer inlet gas changes from 28.6 (vol.%) natural gas and 71.4% steam (molar ratio $M = 2.5$) without anode gas recycling to a mixture consisting of about 17% natural gas, 43% steam, 20% carbon dioxide, 7% carbon monoxide and 13% hydrogen (see [21], p. 434, Table 1, mixture D). The experiments showed that especially the addition of carbon dioxide leads to a strong decrease in catalytic activity of the applied pre-reforming catalyst. In this paper, the influence of anode gas recycling on the performance of SOFC internal methane steam reforming was examined in more detail.

Table 1
Different inlet concentrations of gas mixtures given as partial pressures at $p_{system} = 150$ kPa

Mixture	p_{CH_4} (kPa)	p_{H_2O} (kPa)	p_{H_2} (kPa)	p_{CO_2} (kPa)	p_{CO} (kPa)	p_{N_2} (kPa)
CH_4–H_2O	37.5	112.5	–	–	–	–
Mix A	18.8	56.2	–	–	–	75
Mix B	21.2	50.6	32.6	40.1	5.6	–
Mix C	16.2	47.6	42.8	31.5	12.0	–

3. Experimental

The steam reforming experiments were performed in an apparatus consisting of a gas supply section, an electric furnace and a gas analysis system based on gas chromatography (Hewlett–Packard, HP 5890 Series II) and in parallel on infrared spectroscopy (Fisher–Rosemount, NGA 2000). In the electric furnace the reaction temperature can be adjusted up to 1273 K. The reaction takes place on 1.5 mm thick anode samples with a surface area of 30 mm × 10 mm. The anode cermets were located on a semicylinderical carrier. This construction is placed in a ceramic tube with an inner diameter of 12 mm and a length of about 1 m. Fig. 1 shows a

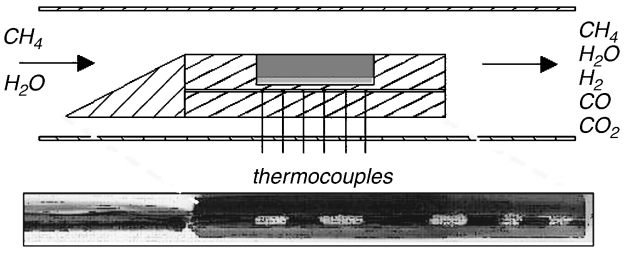

Fig. 1. Experimental set-up for testing the catalytic activity of anode cermets. Test conditions: area velocity: 20–100 $m^3_{N,CH_4}/(m^2\,h)$; velocity: 0.3–2 m/s; molar ratio: 3–7 mol H_2O/mol CH_4; pressure: 150 kPa; furnace temperature: 773–1273 K.

schematic of the experimental set-up. Along the tube five thermocouples are installed at equal distances. The temperature decrease along the cermet caused by the endothermic steam reforming reaction is detected with three thermocouples located inside the sample carrier. For the evaluation, the mean value of the three thermocouples was taken into account resulting in the so-called cermet temperature. The experimental set-up is discussed in more detail in [26,36]. The anode cermet consists of Ni-8YSZ (8 mol.% Y_2O_3-stabilized ZrO_2) substrate with a standard composition of 50% (mass) Ni. They were manufactured by a coat mix process starting with a powder mixture of NiO (56% mass) and 8YSZ together with a resin. More information on the manufacturing process is given by Buchkremer et al. [37]. The anode cermets were reduced in a gas stream consisting of H_2 (5 vol.%) and N_2 in the following steps:

1. heating at 2 K/min until 1073 K is reached;
2. reduction for 2 h at 1073 K;
3. heating at 2 K/min until 1123 K is reached.

4. Results and discussion

4.1. Influence of area velocity and partial pressures of methane and steam

The influence of the partial pressures of methane and water have been discussed thoroughly in the literature [16,17,25,28]. Drescher and co-worker reported that the catalyst activity depends on the partial pressure of methane and water according to a Langmuir–Hinshelwood relation [27,28].

$$r = \frac{kK_{CH_4}p_{CH_4}K_{H_2O}p_{H_2O}}{(1 + K_{CH_4}p_{CH_4} + K_{H_2O}p_{H_2O})^2} \quad (1)$$

These experiments were performed with crushed particles of the anode cermet material. Figs. 2 and 3 show analogous experiments with the 1.5 m thick anode cermets. As can be seen the catalyst activity, i.e. the area-specific methane conversion ($mol_{CH_4}/(m^2\,h)$), increases linearly with increasing methane partial pressure. In parallel to the experiments performed by Drescher varying the methane partial pressure, a maximum conversion which is included in Eq. (1) could not be observed. Additionally, the measured data published by Drescher [28] indicates the influence of methane adsorption on the catalyst surface by the regressive shape of the relation between conversion and partial pressure. Fixing the partial pressure of methane and varying the molar ratio between steam and methane from 3:1 to 7:1 shows a slight decline in catalyst activity. The results are in good agreement with those of Dicks et al. [25]. Considering the measurements of Drescher [28] the maximum catalyst activity exists for a molar ratio of 1:1. At lower partial pressures of water versus those of methane ($M < 1$) the conversion decreases.

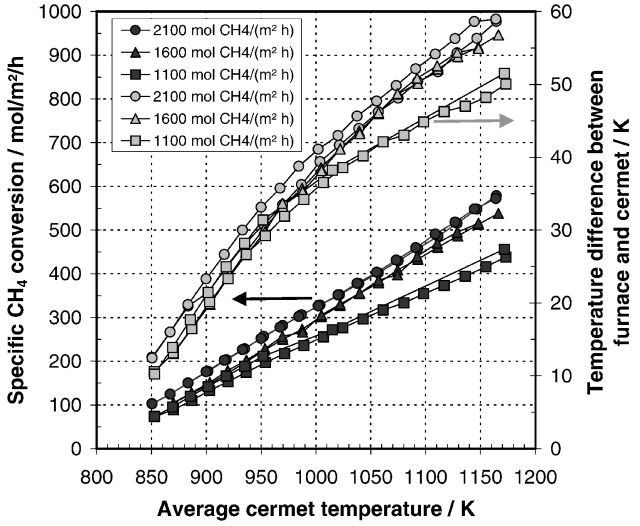

Fig. 2. Specific methane conversion and temperature difference between furnace and cermet as a function of average cermet temperature. Test conditions: area velocity: 1100, 1600 and 2100 $mol_{CH_4}/(m^2\,h)$; $p_{CH_4} = 37.5$ kPa; $p_{H_2O} = 112.5$ kPa.

Another aspect of the experiments is the influence of the gas velocity in the channels above the anode cermet on methane conversion. The inlet methane flow rate was varied between 1100 and 2100 $mol_{CH_4}/(m^2\,h)$. This corresponds to 24.7−47.1 $m^3_{N,CH_4}/(m^2\,h)$ or 100−190 $m^3_N/(m^2\,h)$ at $M = 3$. For a cross-section area of 65.58 mm^2 and a cermet surface of about 390 mm^2 gas velocities of about 0.4 m/s (0.6, 0.8 m/s) are obtained. As can be seen, the experiments only show an influence of the gas velocity between the data for 0.4 (1100 $mol_{CH_4}/(m^2\,h)$) and 0.6 m/s (1600 $mol_{CH_4}/(m^2\,h)$).

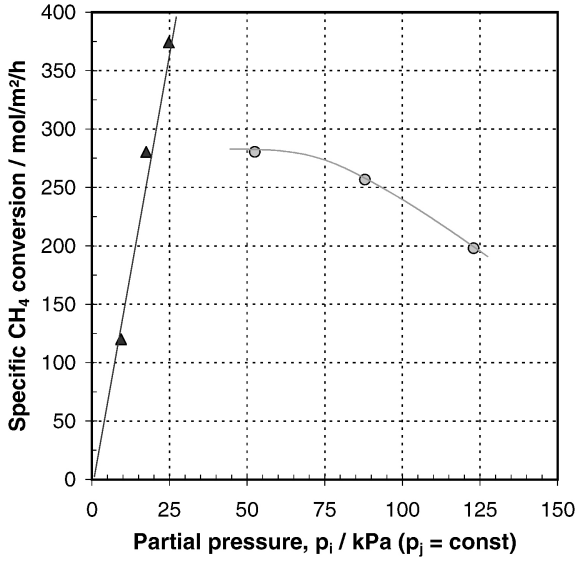

Fig. 3. Specific methane conversion as a function of partial pressure at 1023 K and 150 kPa for a flow rate corresponding to 1340 $mol_{CH_4}/(m^2\,h)$. Partial pressures: (▲) p_{CH_4} on x-axis and $p_{H_2O} = 3p_{CH_4}$; (○) $p_{CH_4} = 18$ kPa and p_{H_2O} on x-axis resulting in $M_{H_2O:CH_4}$ in [3,5,7].

This can be explained by insufficient mass transport from the bulk phase to the boundary layer.

For higher gas velocities the specific methane conversion increases nearly linearly with increasing cermet temperature. For low specific velocities the poorer mass transfer is indicated by a bending of the slope, i.e. conversion versus temperature, at temperatures higher than 1000 K. On the right-hand side, the temperature difference between the furnace temperature and the cermet temperature is shown. It is obvious that the furnace is not able to provide the heat for the endothermic steam reforming reaction by radiation mechanisms to the small surface area. Also it can be expected that for the SOFC stack similar differences in the temperature profile occur. At high temperatures of 1173 K the temperature difference amounts to 50–60 K corresponding to methane conversions between 27 and 40%. At low temperatures of 850 K the methane conversion rate amounts to 5–10% with a temperature difference of about 10 K. At the working temperature of the FZJ substrate concept of 1023 K the temperature difference amounts to about 40 K showing a further advantage of this concept.

4.2. Influence of anode gas recycling

From the balance of plant calculations the concentration behind the pre-reformer can be calculated leading directly to the SOFC anode inlet concentration. The inlet gas consists of 10.8% CH_4, 31.7% H_2O, 21% CO_2, 8% CO and 28.5% H_2 (corresponding to [21], p. 434, Table 1, mixture D). In order to understand the effects of the different gases on the catalyst performance the partial pressures of all components were varied. Nitrogen was supplied as the balance gas to keep the system pressure at 150 kPa.

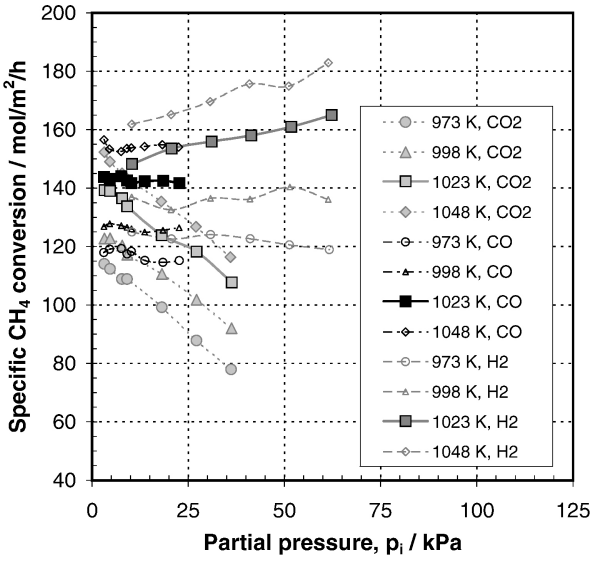

Fig. 4. Effect of individual gases (CO, CO_2, H_2) on catalyst performance. Test conditions: area velocity: 950 $mol_{CH_4}/(m^2\,h)$; $p_{CH_4} = 17.5$ kPa, $p_{H_2O} = 52.5$ kPa.

Fig. 4 shows the area-specific methane conversion as a function of the partial pressures of CO_2, CO, H_2 for four different temperatures of the furnace, i.e. 973, 998, 1023 and 1048 K. The partial pressures of methane and water were kept constant at 17.5 and 52.5 kPa, respectively. As can be seen carbon monoxide has no influence on catalyst performance up to 25 kPa. Likewise, at lower temperatures hydrogen shows no effect on the methane conversion rate, even at elevated temperatures the methane conversion is higher for high hydrogen partial pressures. At 1048 K the specific methane conversion increases from 160 $m^3_{CH_4}/(m^2\,h)$ without the addition of hydrogen to 180 $m^3_{CH_4}/(m^2\,h)$ for a H_2 partial pressure of 60 kPa. This can be explained by a re-reduction of the catalyst by hydrogen if the catalyst has previously displayed some ageing effects. If carbon dioxide is added a strong decrease in the specific methane conversion rate can be observed, i.e. from 145 $m^3_{CH_4}/(m^2\,h)$ without CO_2 addition down to 105 $m^3_{CH_4}/(m^2\,h)$ for a CO_2 partial pressure of 30 kPa.

In order to describe the effect of carbon dioxide an additional term was included in Eq. (1). It is assumed that CO_2 adsorbs on the catalyst surface blocking active sites.

$$r = \frac{kK_{CH_4}p_{CH_4}K_{H_2O}p_{H_2O}}{(1 + K_{CH_4}p_{CH_4} + K_{H_2O}p_{H_2O} + K_{CO_2}p_{CO_2})^2} \quad (2)$$

The kinetic parameters are given by Drescher [28]. The adsorption constant K_{CO_2} is calculated from the specific methane conversion rates determined by experiments in relation to those rates without CO_2 addition.

$$\frac{r(p_{CO_2})}{r(p_{CO_2} = 0\,\text{kPa})} = \frac{\Delta\dot{n}_{CH_4}(p_{CO_2})}{\Delta\dot{n}_{CH_4}(p_{CO_2} = 0\,\text{kPa})} \quad (3)$$

It is assumed that the mass transfer at higher conversion rates is not influenced by the addition of CO_2. After rearrangement Eq. (3) is derived.

$$K_{CO_2} = \frac{1 + K_{CH_4}p_{CH_4} + K_{H_2O}p_{H_2O}}{p_{CO_2}} \left(\sqrt{\frac{r(p_{CO_2} = 0\,\text{kPa})}{r(p_{CO_2})}} - 1 \right) \quad (4)$$

Fig. 5 shows the Arrhenius plot of the calculated constant K_{CO_2}. As can be seen, the relation between K_{CO_2} and the reciprocal value of the cermet temperature is only linear for high partial pressures of carbon dioxide. For this case the temperature dependence of K_{CO_2} would lead to a heat of adsorption of about −125 kJ/mol. Other kinetic models have to be considered in order to describe the effect of CO_2 on the catalyst activity.

In Fig. 6 the specific CH_4 conversion rate is plotted as a function of the reciprocal cermet temperature. Starting with a methane–water mixture ($M = 3$) the rate decreases at 990 K from 230 $m^3_{CH_4}/(m^2\,h)$ down to 125 $m^3_{CH_4}/(m^2\,h)$ by reducing the methane partial pressure from 36 to 18 kPa. The mixtures B, C which correspond to the BOP calculations for anode gas recycling lead to a further reduction down to 80−100 $m^3_{CH_4}/(m^2\,h)$. The inlet compositions of the different gas mixtures are given in Table 1. The effect of anode gas

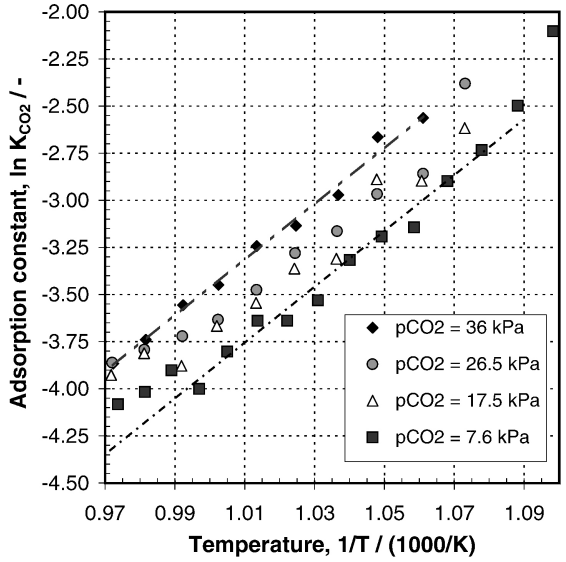

Fig. 5. Arrhenius plot of the adsorption coefficient for four partial pressures of CO_2 according to Langmuir–Hinshelwood. Test conditions: area velocity: 950 $mol_{CH_4}/(m^2\,h)$; $p_{CH_4} = 17.5$ kPa, $p_{H_2O} = 52.5$ kPa.

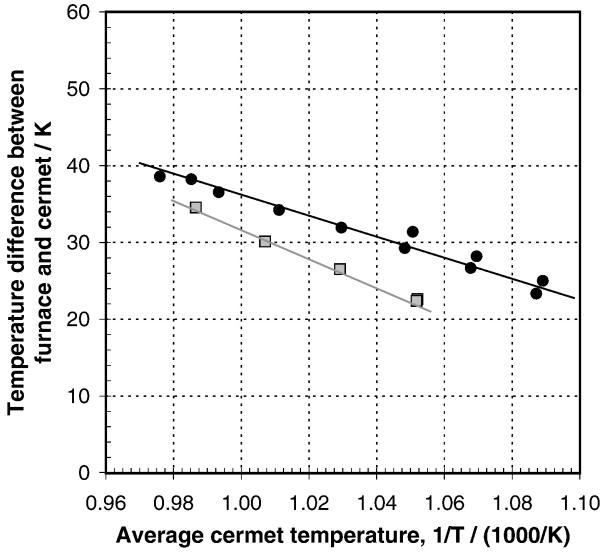

Fig. 7. Temperature difference between furnace and anode cermet as a function of the average cermet temperature with and without anode gas recycling. Area velocity: 550–1100 $mol_{CH_4}/(m^2\,h)$. (●) H_2O–CH_4 ($M = 3$); (■) Mix B; Mix B–C (see Table 1).

recycling increases with decreasing temperature. As can be seen in Fig. 7 the temperature difference between furnace and anode cermet does not change dramatically, i.e. 5–10 K lower for those mixtures assuming anode gas recycling.

An important side reaction concerning steam reforming is the shift reaction, see Eq. (6)

$$CH_4 + H_2O \rightleftharpoons CO + 3H_2 \quad (5)$$

$$CO + H_2O \rightarrow CO_2 + H_2 \quad (6)$$

according to the equilibrium constant:

$$K_{shift} = \frac{p_{CO_2} p_{H_2}}{p_{CO} p_{H_2O}}. \quad (7)$$

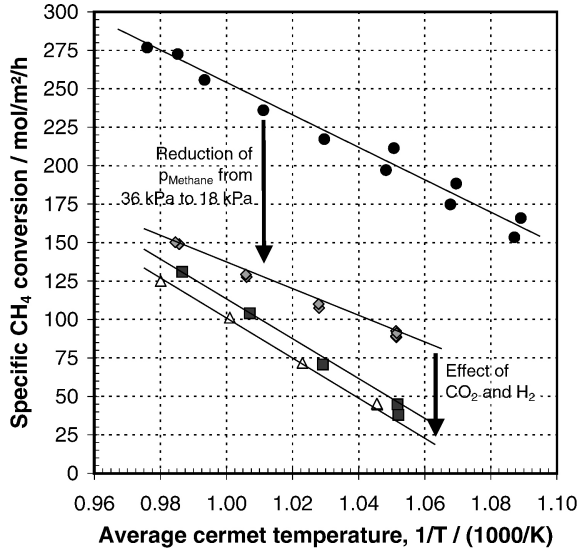

Fig. 6. Arrhenius plot of the specific methane conversion with and without anode gas recycling. Area velocity: 550–1100 $mol_{CH_4}/(m^2\,h)$; (●) H_2O–CH_4 ($M = 3$); (◆) Mix A; (■) Mix B; (△) Mix C; Mix A–C (see Table 1).

In Fig. 8 the equilibrium constant is plotted as an Arrhenius function. The measured reformat composition was used to calculate the distance of the experimental data from the equilibrium values. It is obvious that for the case of standard conditions the CO concentration is higher than that given by the equilibrium composition. This corresponds to a stepwise reaction path of Eqs. (5) and (6), where the shift reaction has not yet reached equilibrium. For a water–methane mixture ($M = 3$) at 1023 K the CO-concentration amounts to about 2.0 vol.% (3.7% CO_2) compared to 1.4% CO (4.5% CO_2) in equilibrium.

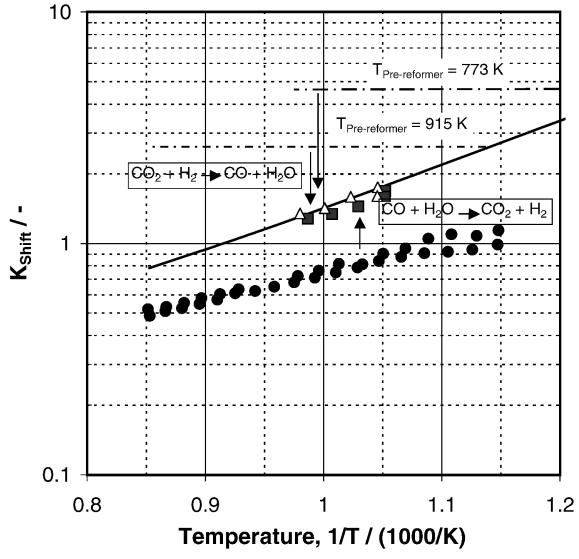

Fig. 8. Shift constant (Eq. (7)) as a function of the average cermet temperature with and without anode gas recycling. Area velocity: 550–1100 $mol_{CH_4}/(m^2\,h)$; (●) H_2O–CH_4 ($M = 3$); (■) Mix B; (△) Mix C; Mix A–C (see Table 1); (—) shift equilibrium.

Assuming anode gas recycling the inlet concentrations for the cermet given by Mix 2 and Mix 3 were adjusted. These values correspond to equilibrium states of a pre-reformer operating at 773 K (Mix 2) and 915 K (Mix 3). As shown in Fig. 8, the calculated shift constant is higher than the equilibrium constant in the advised temperature range for internal reforming. With anode gas recycling 10.9% CO (20% CO_2) was determined at the end of anode cermet. After internal reforming the calculated shift constant was always in equilibrium. Applying anode gas recycling to the reforming process carbon dioxide has to be converted over the anode cermet into carbon monoxide by a reversed CO-shift reaction. This is inverse to the case for standard operation without anode gas recycling whereby, CO is converted into CO_2 by the CO-shift reaction. Although, thermodynamics show that the reaction of CO_2 and CO must follow different directions concerning anode gas recycling or not, this circumstance is no clear explanation for the reduced methane conversion in the case of CO_2-addition while the CO-addition does not influence the methane conversion at all. An oxidation of nickel by carbon dioxide is not expectable due to the presence of hydrogen during the experiments with anode gas recycling. One reason could be, that methane can also be reformed with CO_2 according to:

$$CH_4 + CO_2 \rightleftharpoons 2CO + 2H_2 \quad (8)$$

It might be possible that carbon dioxide and water compete in methane reforming. As shown by Rostrup-Nielson and Bak Hansen [38] carbon dioxide and steam reforming can proceed over the same catalyst. As can be seen from their data, the rate of methane CO_2 reforming on the tested catalysts was lower than that for methane steam reforming, i.e. 30% over Ni/MgO. In order to find a more reliable kinetic model further investigations must be done to describe the effect of methane reforming over Ni/YSZ in the presence of steam and carbon dioxide.

5. Summary

In an SOFC system anode gas recycling can be useful for dispensing with a separate evaporator unit by recycling steam. From earlier measurements concerning a pre-reformer, it is known that the amount of catalyst required is much bigger in the case of anode gas recycling. Assuming anode gas recycling for SOFC-internal steam reforming, the addition of carbon dioxide also leads to a reduction of methane conversion on the anode cermet material NZ41. The effect can be accounted for, roughly by an additional term for CO_2 adsorption in the Langmuir–Hinshelwood kinetics described by Drescher [28]. Further investigations have to be done to find a more reliable kinetic model to describe the CO_2 influence on methane reforming. For design purposes the actual kinetic model can be taken to calculate the influence of CO_2 on the temperature profile across the SOFC.

Acknowledgements

The authors thank B. Sobotta and W. Beckers for technical assistance. They would like to thank J. Meusinger and L.G.J. de Haart for scientific support and valuable discussions.

References

[1] W.L. Lundberg, S.E. Veyo, Conceptual design and performance analysis of a 300 MW_{el} LNG-fuelled pressurised SOFC/Gas turbine power plant, in: H. Yokohawa, S.C. Singhal (Eds.), Proceeding of the 7th International Symposium on Solid Oxide Fuel Cells VII, 2001, pp. 78–87.
[2] R.A. George, J. Power Sources 86 (2000) 134–139.
[3] R. Diethelm, E. Batawi, K. Honegger, in: A. McEvoy (Ed.), Proceedings of the 4th European International Solid Oxide Fuel Cell Symposium, 2000, p. 183.
[4] D. Ghosh, M. Pastula, R. Boersma, D. Prediger, M. Perry, A. Horvath, in: Proceedings of the 2000 Fuel Cell Seminar, Portland, OR, USA, 2000, pp. 511–514.
[5] S. Mukerjee, M.J. Grieve, K. Haltiner, M. Faville, J. Noetzel, K. Keegan, D. Schumann, D. Armstrong, D. England, J. Haller, C. DeMinco, Solid oxide fuel cell auxiliary power unit—a new paradigm in electric supply for transportation, in: H. Yokohawa, S.C. Singhal (Eds.), Proceeding of the 7th International Symposium on Solid Oxide Fuel Cells VII, 2001, pp. 173–179.
[6] N. Minh, A. Anumakonda, R. Doshi, J. Guan, S. Huss, G. Lear, K. Montgomery, E. Ong, J. Yamanis, Portable solid oxide fuel cell system integration and demonstration, in: H. Yokohawa, S.C. Singhal (Eds.), Proceedings of the 7th International Symposium on Solid Oxide Fuel Cells VII, 2001, pp. 155–158.
[7] E. Batawi, U. Weissen, A. Schuler, M. Keller, C. Voisard, Cell manufacturing processes at Sulzer Hexis, in: H. Yokohawa, S.C. Singhal (Eds.), Proceedings of the 7th International Symposium on Solid Oxide Fuel Cells VII, 2001, pp. 140–147.
[8] R.C. Huiberts, J.P.P. Huijsmans, Pilot production of planar SOFC components at InDEC Ltd., in: H. Yokohawa, S.C. Singhal (Eds.), Proceedings of the 7th International Symposium on Solid Oxide Fuel Cells VII, 2001, pp. 155–158.
[9] L.G.J. de Haart, K. Mayer, U. Stimming, I.C. Vinke, J. Power Sources 71 (1998) 302–305.
[10] D. Ghosh, E. Tang, M. Perry, D. Prediger, M. Pastula, R. Boersma, Status of SOFC developments at Global Thermoelectric Ltd., in: H. Yokohawa, S.C. Singhal (Eds.), Proceedings of the 7th International Symposium on Solid Oxide Fuel Cells VII, 2001, pp. 100–109.
[11] G. Rietveld, P. Nammensma, J.P. Ouweltjes, Status of SOFC development at ECN, in: H. Yokohawa, S.C. Singhal (Eds.), Proceedings of the 7th International Symposium on Solid Oxide Fuel Cells VII, 2001, pp. 125–130.
[12] F.J. Gardner, M.J. Day, N.P. Brandon, M.N. Pashley, M. Cassidy, J. Power Sources 86 (2000) 122–129.
[13] B. Godfrey, K. Föger, R. Gillespie, R. Bolden, S.P.S. Badwal, J. Power Sources 86 (2000) 68–73.
[14] L.G.J. de Haart, I.C. Vinke, A. Janke, H. Ringel, F. Tietz, New developments in stack technology for anode substrate based SOFC, in: H. Yokohawa, S.C. Singhal (Eds.), Proceedings of the 7th International Symposium on Solid Oxide Fuel Cells VII, 2001, pp. 111–119.
[15] J.R. Rostrup-Nielsen, Catalytic Steam Reforming, Springer, Berlin, 1984.
[16] A.L. Dicks, J. Power Sources 71 (1998) 111–122.
[17] J. Meusinger, E. Riensche, U. Stimming, J. Power Sources 71 (1/2) (1998) 315–320.

[18] M. Pastula, J. Devitt, R. Boersma, D. Ghosh, Fuel processing development at Global Thermoelectric Ltd., in: H. Yokohawa, S.C. Singhal (Eds.), Proceedings of the 7th International Symposium on Solid Oxide Fuel Cells VII, 2001, pp. 180–190.
[19] C. Finnerty, G.A. Tompsett, K. Kendall, R.M. Ormerod, J. Power Sources 86 (2000) 459–463.
[20] S. Freni, G. Calogero, S. Cavallero, J. Power Sources 87 (2000) 28–38.
[21] R. Peters, E. Riensche, P. Cremer, J. Power Sources 86 (2000) 432–441.
[22] C.M. Finnerty, R.M. Ormerod, J. Power Sources 86 (2000) 390–394.
[23] W. Lehnert, J. Meusinger, F. Thom, J. Power Sources 87 (2000) 57–63.
[24] Ch. Rechenauer, E. Achenbach, Internal Report of Forschungszentrum Jülich, IEV, Jül-2752, 1993.
[25] A.L. Dicks, K.D. Pointon, A. Siddle, J. Power Sources 86 (2000) 523–530.
[26] E. Achenbach, E. Riensche, J. Power Sources 52 (1994) 283–288.
[27] R. Peters, I. Drescher, J. Meusinger, Kinetics of methane steam reforming, in: Proceedings of the 2000 Fuel Cell Seminar, Portland, OR, USA, 2000, 305–308.
[28] I. Drescher, Ph.D. Thesis, RWTH Aachen, 1999.
[29] M.B. Joerger, L.J. Gauckler, Catalytically active anodes for SOFC, in: H. Yokohawa, S.C. Singhal (Eds.), Proceedings of the 7th International Symposium on Solid Oxide Fuel Cells VII, 2001, pp. 671–677.
[30] P. Aguiar, R. Ramírez-Cabrera, A. Atkinson, Catalyt configurations for indirect internal steam reforming in SOFC's, in: H. Yokohawa, S.C. Singhal (Eds.), Proceedings of the 7th International Symposium on Solid Oxide Fuel Cells VII, 2001, pp. 703–711.
[31] T. Ishihara, Y. Tsuruta, H. Nishiguchi, Y. Takita, New internal reforming $LaGaO_3$ solid oxide fuel cell based on partial oxidation of methane, in: Proceedings of the 2000 Fuel Cell Seminar, Portland, OR, USA, 2000, pp. 550–553.
[32] S.J.A. Livermore, J.W. Cotton, R.M. Ormerod, J. Power Sources 86 (2000) 411–416.
[33] E. Riensche, J. Meusinger, U. Stimming, G. Unverzagt, J. Power Sources 71 (1998) 306–314.
[34] E. Riensche, U. Stimming, G. Unverzagt, J. Power Sources 73 (1998) 251–256.
[35] G. Unverzagt, Ph.D. Thesis, RWTH Aachen, 1995.
[36] W. Lehnert, J. Meusinger, E. Riensche, U. Stimming, in: B. Thorstensen (Ed.), Proceedings of the 2nd European SOFC Forum, Oslo, Norway, 1996, pp. 143–152.
[37] H.P. Buchkremer, U. Diekmann, D. Stöver, in: S.C. Singhal, U. Stimming, H. Tagawa, W. Lehnert (Eds.), Proceedings of the 5th International Symposium on Solid Oxide Fuel Cells, The Electrochemical Society, Pennington, NJ, 1997, pp. 40–97, 993.
[38] J.R. Rostrup-Nielsen, J.H. Bak Hansen, J. Catal. 144 (1993) 38–49.